Crystallographic inversion-mediated superparamagnetic relaxation in Zn-ferrite nanocrystals

Cite as: AIP Advances **10**, 015101 (2020); https://doi.org/10.1063/1.5130483
Submitted: 04 October 2019 . Accepted: 16 November 2019 . Published Online: 02 January 2020

Ranajit Sai, Sarath Arackal, R. D. Ralandinliu Kahmei, Navakanta Bhat, Masahiro Yamaguchi, and S. A. Shivashankar

Crystallographic inversion-mediated superparamagnetic relaxation in Zn-ferrite nanocrystals

Cite as: AIP Advances 10, 015101 (2020); doi: 10.1063/1.5130483
Presented: 8 November 2019 • Submitted: 4 October 2019 •
Accepted: 16 November 2019 • Published Online: 2 January 2020

Ranajit Sai,[1,a] Sarath Arackal,[1] R. D. Ralandinliu Kahmei,[1] Navakanta Bhat,[1] Masahiro Yamaguchi,[2] and S. A. Shivashankar[1]

AFFILIATIONS

[1]Centre for Nano Science and Engineering, Indian Institute of Science, Bengaluru 560012, Karnataka, India
[2]Dept. of Electrical Engineering, Tohoku University, Sendai 980-8579, Miyagi, Japan

Note: This paper was presented at the 64th Annual Conference on Magnetism and Magnetic Materials.
[a]**Corresponding author:** ranajit@ieee.org

ABSTRACT

Crystallographic inversion induced shift of resonance frequency in zinc ferrite nanoparticle (ZF-NP) samples is studied here. ZF-NP samples were synthesized by a solution-based, low-temperature (<200 °C), microwave-assisted solvothermal (MAS) process. Owing to the far-from-equilibrium processing condition, the MAS process produces a very high degree of crystallographic inversion, δ=0.61, in the as-synthesized nanocrystallites. A rapid thermal annealing (RTA) technique was adopted to tune-down crystallographic inversion without altering the crystallite sizes in annealed samples. The crystal structures, particle shapes, and compositions of the nanocrystalline samples were characterized by XRD, SEM and Raman spectroscopy. The samples are phase-pure, with particle size in the range 8-16 nm and their compositions are stoichiometrically accurate. The resonance phenomena in 1 to 10 GHz frequency range was measured by analyzing the impedance mismatch of a microstrip line with the magnetic material loaded on to it. The RTA protocol enables tuning of the resonance phenomena in the ZF-NC samples above 6 GHz with tunable range of ~500 MHz

I. INTRODUCTION

Superparamagnetic relaxation (SR) is an important feature of the nanocrystalline ferrite particles in view of their applications in microwave frequencies.[1,2] Owing to their very small volume (V_p), magnetic nanocrystallites often possess magnetic anisotropy energy (KV_p; K: anisotropy constant) comparable to the thermal energy (k_BT). This condition results in magnetization reversal triggered by thermal fluctuation at a certain temperature, T. As the frequency dependence of magnetic susceptibility of a single-domain superparamagnetic particle depends on the ratio of the anisotropy energy and thermal energy, the imaginary part of susceptibility, $\chi''(f)$, peaks at a frequency, $f_{SR} = 1/\tau = f_0 e^{-KV_p/k_BT}$, known as superparamagnetic/ferrimagnetic relaxation rate.[3] It increases with decreasing particle volume, known as nano-size-effect. Therefore, tuning of SR frequency can play a great role in extending the applicability of ferrite nanocrystallites beyond their natural resonance frequency.[2]

Resonance phenomena in a nanocrystalline material often observes at a higher frequency than reported in their bulk form.[2,4–6] This is attributed to the aforesaid nano-size-effect. While the effect of magnetic core-shell,[2,7–9] particle size and shape,[10–12] etc on SR process was investigated, the effect of crystallographic inversion – the nonequilibrium distribution of cations in a spinel lattice – is explored less often.[13,14] Moreover, achieving a high degree of inversion, δ>0.2, is a daunting task.[14] Recently, zinc ferrite nanocrystallites prepared by a kinetically-driven, far-from-equilibrium synthesis process – microwave-irradiation assisted solvothermal (MAS) process – result in a very high degree of inversion (δ~0.5).[15] Thin ferrite films deposited by the aforesaid MAS process enhanced

inductance and quality factor of an on-chip inductor above 6 GHz.[16,17] However, the effect of such a high degree of inversion on relaxation process in microwave frequency regime was never investigated.

Here we have measured the relaxation frequency of four zinc ferrite nanocrystalline sample having δ ranging from 0.49 to 0.61 to explore the effect of inversion on SR process. Furthermore, we have demonstrated controlled decrease of inversion without altering the crystallite size by fine-tuning a rapid thermal annealing protocol.

II. EXPERIMENTS

Zinc ferrite powder samples were prepared by a two-step process as depicted in the schematic diagram of Fig. 1 (a). The first step is the MAS process that produces the stock unannealed (UA) sample, which then is subjected to the RTA process to transform into three anneal samples – RA41, RA42, and RA44. The processing parameters of the MAS and RTA processes are shown in Fig. 1 (b) and (c) respectively.

In a typical MAS process, stoichiometric quantity of metal-organic precursors - $Zn(acac)_2$ (Zinc acetylacetonate) and $Fe(acac)_3$ (Iron acetylacetonate) were dissolved in an ethanol/1-decanol solvent mixture (3:5 volume ratio) before exposing the mixed solution under microwave (2.45 GHz, 300 W) irradiation (Discover, CEM Corp., US). After irradiation, the solution was then cooled to room temperature allowing the precipitates to settle. The solid precipitate was separated by centrifugation (15 min at 6000 rpm) and washed repeatedly with ethanol and acetone to remove unreacted precursors if any. The precipitate was then dried at 50 °C for 24 hours and subsequently grounded to fine powder using mortar and pestle. A good yield of >98% was obtained, which was then taken for RTA process.

Rapid thermal annealing of the zinc ferrite powder was done at 400°C for three different annealed time (1 min (RA41), 2 mins (RA42), and 4 mins (RA44)) using MILA-5000 system (ULVAC, Japan) (Fig. 1c). The samples (UA, RA41, RA42, RA44) were made into pellets of 10 mm diameter and are taken for further characterization.

The crystal structure, lattice parameter and average crystallite size of the samples were analyzed by X-Ray diffractometer (CuKα, Rigaku SmartLab). The shape of the nanocrystallites was analyzed using Scanning Electron Microscope (SEM) (Ultra 55, Gemini technology). The vibrational modes and inversion parameters were examined at room temperature (300 K) by Raman Spectroscopy (LabRam HR, Horiba). A 3.2 mW, 532 nm laser was used as an excitation source with an integration time 10 s for one round of data acquisition. Such 50 acquisitions were done to improve the signal to noise ratio. The high-frequency magnetic behavior of the samples was measured using a microstrip line (MSL) method by exploiting the impedance mismatch caused by materials with different magnetic property. The pellet samples were placed over a 50 Ω microstrip line and the s-parameters were measured using a vector network analyzer (VNA), Agilent technologies (E8361A) in the frequency range 1 to 10 GHz.

III. RESULT AND DISCUSSION

XRD patterns of the as-prepared and annealed samples are shown in Fig. 2. The as-prepared sample (UA, Fig. 2a) shows broader peaks, a characteristic of very small crystals, and elucidates distinct sharpening of the diffraction peaks of RA41, RA42, and RA44 – attesting improved crystallinity and thus grain growth. The diffraction patterns can be indexed to cubic zinc ferrite, $ZnFe_2O_4$ (ICDD No.: 01-073-1963). The average crystallite size (D) of all the annealed samples are found to be near identical (15.5 ± 0.6 nm), whereas it's about 8.5 nm in the unannealed sample. A variation in lattice parameter (*a*) is also observed within annealed samples.

SEM images (Fig. 3) clearly reveal the crystal growth in annealed samples compared to the UA sample. However, the shape and size of the annealed samples are similar to each other. Therefore,

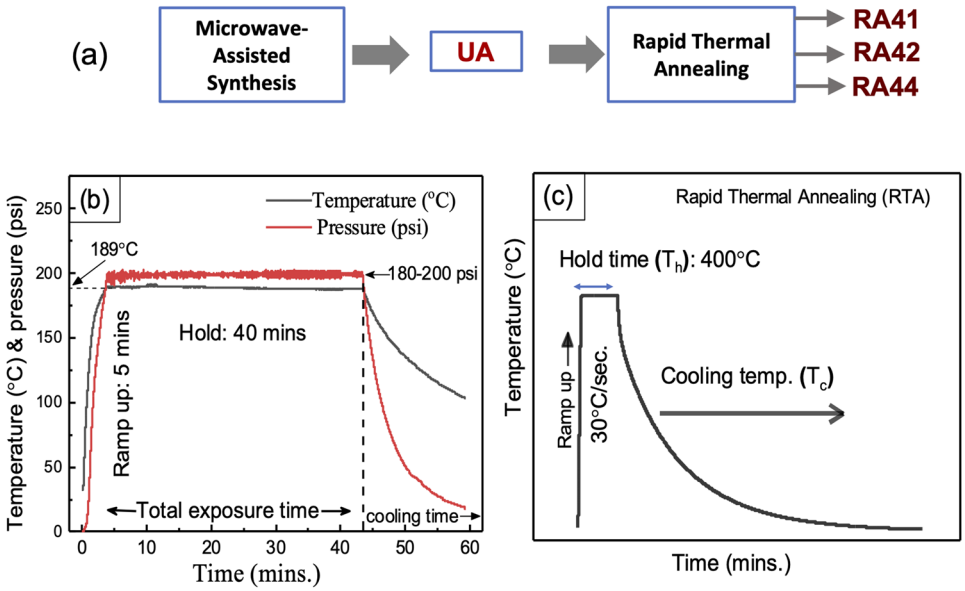

FIG. 1. (a) Block-diagram of the sample preparation steps; (b) and (c) Depiction of various process parameters of MAS and RTA processes respectively.

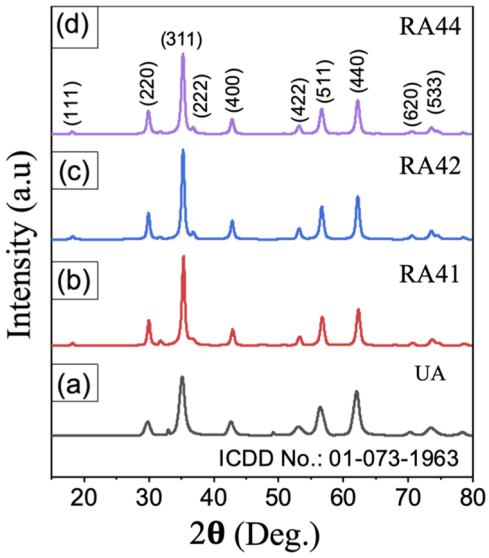

FIG. 2. X-Ray Diffraction patterns of various samples; (a) UA, (b) RA41, (c) RA42, and (d) RA44.

the variation in lattice parameter cannot be attributed to the particle size and shape. Due to their different ionic radius, redistribution of cations in the lattice system can induce alteration in their structural parameters such as a and u (oxygen parameter).

This indicates that the overall magnetic anisotropy energy in all annealed samples will be in same order because their particle volume is almost same and shape-induced anisotropy of them are also comparable. Since the f_{SR} depends on the magnetic anisotropy, the annealed samples - RA41, RA42, RA44, which have similar size and shape, hence similar anisotropy, are good candidates to study the dependence of inversion-induced anisotropy on f_{SR}.

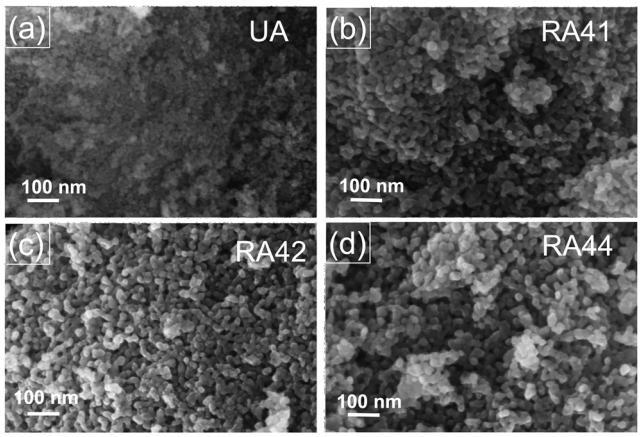

FIG. 3. SEM of various samples; (a) UA, (b) RA41, (c) RA42, and (d) RA44.

The cubic spinel structure with space group Fd-3m exhibits five characteristic Raman modes, namely A_{1g}, E_g, and three T_{2g} corresponding to the symmetric and asymmetric bending or stretching of oxygen ions with the metal ions.[18] Room temperature Raman spectra of zinc ferrite nanoparticles are shown in Fig. 4. All the samples exhibit the characteristic peaks reported in various literature.[19–21] The A_{1g} broad peaks observed at ~560-700 cm^{-1} is attributed to the symmetric stretch in the tetrahedral site (A-site). Therefore, the A_{1g} peaks were de-convoluted by fitting them with individual Gaussian-Lorentzian components to identify the occupying cations in A-site. The deconvoluted peaks in zinc ferrite nanocrystals appearing at 618 cm^{-1} and 666 cm^{-1} correspond to tetrahedrally coordinated Zn-O and Fe-O stretches respectively. Therefore, the presence of Fe^{3+} ions at A-sites in zinc ferrite indicates the structural transformation of a typical normal spinel to a partially inverse spinel system.

Since A_{1g} Raman mode is associated with the stretching vibration of the ion species in the A-site, the integrated intensity of A_{1g} mode is then proportional to the Zn_A and Fe_A content in the A-site respectively.[22] The cation re-distribution between the A- and B-sites were estimated from the area under the deconvoluted peaks indicated in Fig 4. An unprecedentedly high percentage of Fe^{3+} ions were found in A-site (61%) of unannealed sample contrary to the bulk condition wherein it should be zero. The inversion parameter for UA is close to the value predicted by Sai *et al.*[15] Moreover, it is important to note that the degree of inversion can be tuned from 0.61 to 0.49 by rapid thermal annealing. Hence, RTA appears to be an excellent technique to tune the inversion in spinel ferrite.

Now, it is apparent from the SEM and XRD measurements that the shape and size induced anisotropy is identical for the

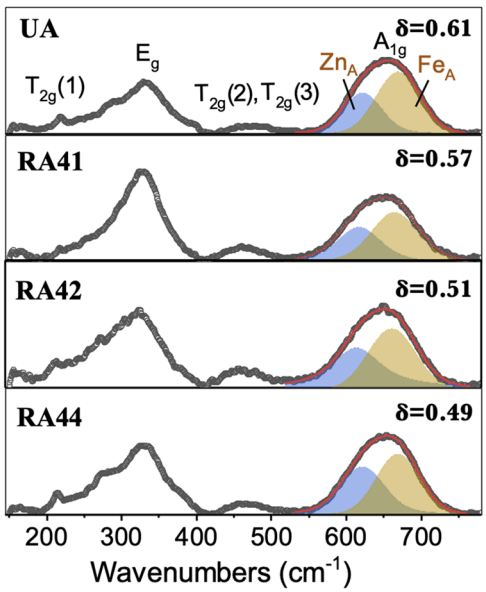

FIG. 4. Analysis of Raman-modes of unannealed (UA) and annealed (RA41, RA42, and RA44) zinc ferrite samples highlighting the presence of crystallographic inversion in them.

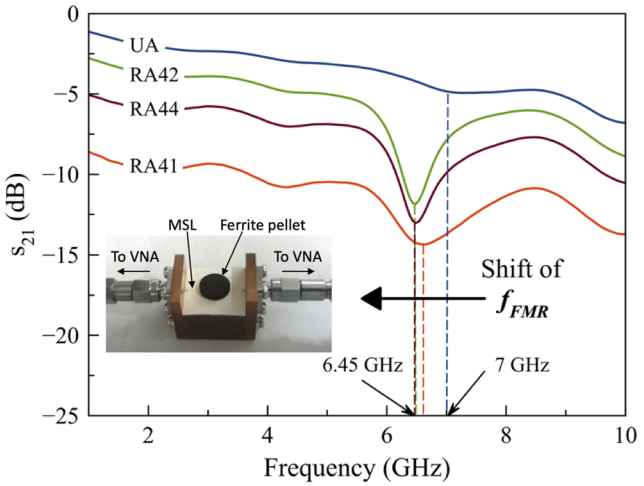

FIG. 5. Transmission characteristics of a impedance-matched microstrip line (MSL) loaded with powder pellets of zinc ferrite samples; (in inset) photograph of the measurement fixture with a pellet on top of MSL.

annealed samples presented here. Since there is a significant change in the inversion due to RTA, it is expected that the superparamagnetic resonance frequency (f_{SR}) of the annealed samples will be different.[13] This change in f_{SR} can be attributed to the inversion-induced anisotropy of the samples, which otherwise have similar magneto-crystalline anisotropy.

To test this hypothesis, we employ an MSL based approach where we study the material response by probing the impedance mismatch in the microstrip line when the magnetic samples occupy the dielectric medium over it. The transmission parameter (s_{21}) of the MSL loaded with various ferrite pellets are shown in Fig. 5. A noticeable dip in s_{21} is observed in between 6 to 7 GHz for all samples that can be attributed to the loss stemming from the imaginary part of the complex susceptibility of the material. For unannealed sample (UA, with the highest inversion, δ=0.61) the dip occurs at 7 GHz, which then gradually shifted to 6.45 GHz for which the inversion was smallest among the measured samples. Therefore, by employing the RTA protocol adopted here, one can tune the resonance phenomena above 6 GHz with tunable range of ~500 MHz.

IV. CONCLUSION

The effect of crystallographic inversion on the superparamagnetic/ferrimagnetic relaxation process in zinc ferrite nanoparticle (ZF-NP) samples was investigated. ZF-NP samples were synthesized by a solution-based, low-temperature (<200 °C), microwave-assisted solvothermal (MAS) process and possess an unprecedently high degree of crystallographic inversion (δ=0.61) in the as-synthesized nanocrystallites. A rapid thermal annealing (RTA) technique was adopted to tune-down crystallographic inversion without altering the crystallite sizes in annealed samples. The samples are phase-pure, with particle size in the range 8-16 nm and their compositions are stoichiometrically accurate. The resonance frequency of the unannealed sample turns out to be 7 GHz. The RTA protocol enables tuning of the resonance phenomena in the ZF-NC samples above 6 GHz with tunable range of ~500 MHz.

ACKNOWLEDGMENTS

The authors are thankful to MNCF (Micro Nano Characterization Facility), CeNSE, IISc, for the instrumentation facility, and ISRO, Dept. of Space, Govt. of India for the partial financial support to the project. It is also supported partially by the DST-JSPS joint bilateral research project.

REFERENCES

[1] V. G. Harris, IEEE Trans. Magn. **48**, 1075 (2012).
[2] N.-N. Song, H.-T. Yang, H.-L. Liu, X. Ren, H.-F. Ding, X.-Q. Zhang, and Z.-H. Cheng, Sci. Rep. **3**, 3161 (2013).
[3] W. F. Brown, Phys. Rev. **130**, 1677 (1963).
[4] D. Guo, Z. Zhang, M. Lin, X. Fan, G. Chai, Y. Xu, and D. Xue, J. Phys. D. Appl. Phys. **42**, 125006 (2009).
[5] A. K. Subramani, K. Kondo, M. Tada, M. Abe, M. Yoshimura, and N. Matsushita, Mater. Chem. Phys. **123**, 16 (2010).
[6] M. Hofmann, S. J. Campbell, H. Ehrhardt, and R. Feyerherm, J. Mater. Sci. **39**, 5057 (2004).
[7] T. Ahmad, H. Bae, I. Rhee, Y. Chang, J. Lee, and S. Hong, Curr. Appl. Phys. **12**, 969 (2012).
[8] Y. D. Zhang, J. I. Budnick, W. A. Hines, C. L. Chien, and J. Q. Xiao, Appl. Phys. Lett. **72**, 2053 (1998).
[9] V. Blanco-Gutiérrez, M. J. Torralvo-Fernández, and R. Sáez-Puche, J. Phys. Chem. C **114**, 1789 (2010).
[10] Y. Jun, Y. Huh, J. Choi, J. Lee, H. Song, S. Kim, S. Yoon, K. Kim, J. Shin, J. Suh, and J. Cheon, J. Am. Chem. Soc. **127**, 5732 (2005).
[11] P. van der Zaag, V. Brabers, M. Johnson, A. Noordermeer, and P. Bongers, Phys. Rev. B **51**, 12009 (1995).
[12] V. Blanco-Gutierrez, R. Saez-Puche, and M. J. Torralvo-Fernandez, J. Mater. Chem. **22**, 2992 (2012).
[13] A. Yang, Z. Chen, S. M. Islam, C. Vittoria, and V. G. Harris, J. Appl. Phys. **103**, 07E509 (2008).
[14] V. G. Harris and V. Šepelák, J. Magn. Magn. Mater. **465**, 603 (2018).
[15] R. Sai, S. D. Kulkarni, S. S. M. Bhat, N. G. Sundaram, N. Bhat, and S. A. Shivashankar, RSC Adv. **5**, 10267 (2015).
[16] R. Sai, S. D. Kulkarni, M. Yamaguchi, N. Bhat, and S. A. Shivashankar, IEEE Magn. Lett. **8**, 1 (2017).
[17] R. Sai, R. D. Ralandinliu Kahmei, S. A. Shivashankar, and M. Yamaguchi, IEEE Trans. Magn. **55**, 1 (2019).
[18] S. W. da Silva, F. Nakagomi, M. S. Silva, A. Franco, V. K. Garg, A. C. Oliveira, and P. C. Morais, J. Nanoparticle Res. **14**, 798 (2012).
[19] J. P. Singh, R. C. Srivastava, H. M. Agrawal, and R. Kumar, J. Raman Spectrosc. **42**, 1510 (2011).
[20] S. Thota, S. C. Kashyap, S. K. Sharma, and V. R. Reddy, J. Phys. Chem. Solids **91**, 136 (2016).
[21] D. Varshney, K. Verma, and A. Kumar, Mater. Chem. Phys. **131**, 413 (2011).
[22] F. Nakagomi, S. W. Silva, V. K. Garg, A. C. Oliveira, P. C. Morais, and A. Franco, Jr., J. Solid State Chem. **182**, 2423 (2009).